Charge transfer degree and superconductivity of the incommensurate organic superconductor $(MDT\text{-}TSF)(I_3)_{0.422}$

Tadashi Kawamoto and Takehiko Mori
Department of Organic and Polymeric Materials, Graduate School of Science and Engineering, Tokyo Institute of Technology, O-okayama, Meguro-ku, Tokyo 152-8552, Japan

Takako Konoike, Kengo Enomoto, Taichi Terashima, and Shinya Uji
National Institute for Materials Science, Tsukuba, Ibaraki 305-0003, Japan

Hiroshi Kitagawa
Department of Chemistry, Faculty of Science, Kyushu University, Hakozaki, Higashi-ku, Fukuoka 812-8581, Japan

Kazuo Takimiya and Tetsuo Otsubo
Department of Applied Chemistry, Graduate School of Engineering, Hiroshima University, Kagamiyama, Higashi-Hiroshima, Hiroshima 739-8527, Japan

(Received 16 November 2005; revised manuscript received 7 February 2006; published 24 March 2006)

The influence of a small change of carrier number on the superconducting transition temperature T_c in the incommensurate organic superconductors is investigated for $(MDT\text{-}TSF)(I_3)_{0.422}$ (MDT-TSF: methylenedithiotetraselenafulvalene, T_c=4.9 K) in comparison with $(MDT\text{-}TSF)(AuI_2)_{0.436}$ (T_c=4.5 K). Careful estimation of the degree of charge transfer by means of the Raman spectra as well as the Shubnikov–de Haas (SdH) oscillations indicates that the charge-transfer degree 0.422 for the I_3 salt is obviously smaller than 0.436 in the AuI_2 salt. According to the band calculation, the former salt has smaller density of states. However, the former salt exhibits higher T_c than the latter compounds, and this disagrees with the naive prediction of the BCS theory. The former salt shows considerably large effective cyclotron mass extracted from the SdH oscillations. These observations demonstrate that the strength of the many-body effect is the major factor that determines T_c in these organic superconductors.

DOI: 10.1103/PhysRevB.73.094513 PACS number(s): 74.70.Kn, 74.25.Jb, 71.18.+y

I. INTRODUCTION

In many organic superconductors, the ratio of the donor molecules to the anions is represented by an integer, such as, typically, 2:1.[1,2] The band filling of these compounds is 3/4-filling, and this corresponds to effective half-filling in the presence of the dimerization gap. The donor/anion ratio takes a definite number for a given combination of donor and anion, and the ratio is not variable, as in many inorganic compounds such as high-T_c cuprate superconductors, in which the ground state is controlled by the carrier number. The ground states of organic compounds are regulated by the bandwidth by means of, for example, pressure.

Several groups have attempted to control the degree of charge transfer; i.e., band filling of organic conductors.[3] The first method to control the charge transfer degree in organic conductors is introducing composite anions of X^- and Y^{2-}, for example, $GaCl_4^-$ and $CoCl_4^{2-}$; these types of conductors change from a band insulator to a metallic conductor, but do not show superconductivity.[4–6] Yamamoto *et al.* have used another approach; they have obtained several materials with unusual donor/anion ratio by mixing neutral molecules with the anions.[7] They have not obtained a superconductor either.

The use of incommensurate crystals is the third way to obtain organic superconductors with unusual band fillings. $(MDT\text{-}TSF)(AuI_2)_{0.436}$ is an organic superconductor categorized in this group, where MDT-TSF is methylenedithiotetraselenafulvalene [Fig. 1(a)].[8] In this superconductor, we have found an incommensurate anion structure and unique Fermi surface reconstruction by the incommensurate anion potential.[9–11] Consequently, the band filling deviates from the usual 3/4-filling and is 0.782. The salts of the sulfur analog MDT-ST, where MDT-ST is 5*H*-2-(1,3-dithiol-2-ylidene)-1,3-diselena-4,6-dithiapentalene, have similar incommensurate structures, and also show superconductivity at ambient pressure.[12–14] Moreover, another

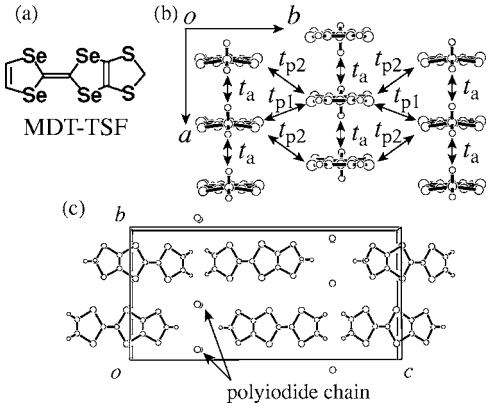

FIG. 1. (a) MDT-TSF molecule. (b) Crystal structure projected along the molecular long axis and (c) projection onto the *bc* plane of $(MDT\text{-}TSF)(I_3)_{0.422}$.

sulfur derivative (MDT-TS)$(AuI_2)_{0.441}$, where MDT-TS is 5*H*-2-(1,3-diselenol-2-ylidene)-1,3,4,6-tetrathiapentalene, undergoes a superconducting transition under high pressure.[15,16] To our knowledge, the MDT-TSF series salts are the only organic incommensurate crystals showing superconductivity based on an asymmetric donor molecule, though ambient pressure superconductivity has been reported in another nonstoichiometric compound κ-$(ET)_4Hg_{2.89}Br_8$ [ET: bis(ethylenedithio)tetrathiafulvalene] based on a symmetric donor molecule.[17]

MDT-TSF superconductors have a uniform donor stacking along the *a* axis and the donors form a conducting sheet on the *ab* plane [Figs. 1(b) and 1(c)]. The crystallographic *c* axis is perpendicular to the *ab* plane, because the crystal system is orthorhombic. We have carried out detailed investigations for the iodide salt of MDT-TSF. Although the x-ray oscillation photograph and the elemental analysis have given us the composition as (MDT-TSF)$I_{1.266}$,[18] we cannot determine the degree of charge transfer, because iodide exists in the forms of I^-, I_2, I_3^-, and I_5^- in solids.[19] (MDT-TSF)$I_{1.266}$ has a possibility in which the charge-transfer degree is different from (MDT-TSF)$(AuI_2)_{0.436}$. Therefore, (MDT-TSF)$I_{1.266}$ is an important material to investigate the effect of charge-transfer degree on superconductivity.

The present paper reports physical properties of the organic superconductor (MDT-TSF)$(I_3)_{0.422}$. The charge-transfer degree is determined precisely from the Raman investigations. The Shubnikov–de Haas (SdH) oscillations also give us the charge-transfer degree, which supports the results based on the Raman investigations. The superconducting properties are also shown. Finally, we propose that the effective cyclotron mass enhancement is related to the superconducting transition temperature T_c in the MDT-TSF superconductors. The density of states estimated from the band calculation is, however, smaller with increasing T_c, suggesting that the many-body effect is important for determining T_c.

II. EXPERIMENT

Single crystals were prepared by electrocrystallization.[18] Raman spectra were measured by He-Ne laser excitation (λ=632.8 nm) using a single monochromator with a supernoch-filter and a microscope. Detection of the scattered radiation was by a Princeton charge-coupled device camera system operated at a temperature of 153 K. Laser power beamed at the crystal was held at $<$20 μW to avoid laser damage. Wave-number calibration was effected by referring to the emission spectrum of a Ne lamp.

The band structure was calculated on the basis of the extended Hückel method and the tight-binding approximation.[20,21] The transfer integrals t_i are estimated from the intermolecular overlap integrals S_i as $t_i=ES_i$, in which the energy level of the highest occupied molecular orbital E is taken to be -10 eV, and the interaction modes (a, $p1$, and $p2$) are defined in Fig. 1(b). The same atomic-orbital parameters as those of (MDT-TSF)$(AuI_2)_{1.266}$ were used.

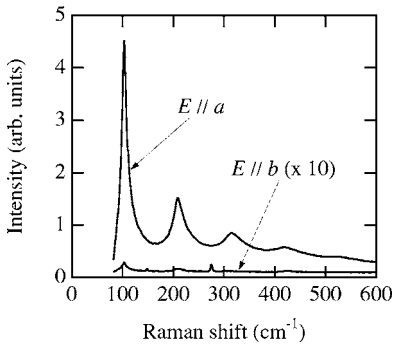

FIG. 2. The Raman spectra of (MDT-TSF)$(I_3)_{0.422}$ measured for polarization $\|a$ and $\|b$ axes at room temperature.

For the SdH measurements, the samples were mounted on a one-axis rotator in the dilution refrigerator in a 20 T superconducting magnet, and the measurements were carried out by the four-probe method along the *a* axis with ac current (1 mA) down to 50 mK. Lock-in amplifiers and preamplifiers were used for the highly sensitive detection.

For the magnetoresistance measurements above 1.6 K, the samples were mounted on a two-axis rotator in a cryostat in a 14 T superconducting magnet. The measurements were carried out by the four-probe method along the *a* axis with dc current (100 μA).

All magnetoresistance measurements were carried out at Tsukuba Magnet Laboratories, NIMS.

III. RESULTS

Figure 2 shows the Raman spectra of (MDT-TSF)$I_{1.266}$ at room temperature. The Raman lines in the $E\|a$ spectrum consist of the 104 cm^{-1} peak and its overtones, and the spectrum shows neither a peak at 160 cm^{-1} originating in the linear I_5^-, nor a shoulder around 145 cm^{-1} coming from the asymmetric stretching mode of discrete I_3^-.[19] This demonstrates that the polyiodide chain is composed of I_3^- units. The observed Raman shift at around 100 cm^{-1} is known as the symmetric stretching mode of I_3^- in an infinite linear chain. On the other hand, the *b*-parallel spectrum shows no Raman line originating in the iodide anion. These observations indicate the existence of the iodide chain running along the *a* axis.

The chemical formula (MDT-TSF)$I_{1.266}$ given by the previous results of the x-ray oscillation photograph and the elemental analysis should be interpreted to be (MDT-TSF)$(I_3)_{0.422}$. The obtained charge-transfer degree (ρ=0.422) is slightly smaller than that of (MDT-TSF)$(AuI_2)_{0.436}$. This is explained by the crystal structure and the anion length. The *a* axis of the donor lattice of the I_3 salt [4.013(4) Å] is the same as that of the AuI_2 salt [4.016(6) Å]. On the other hand, the length of I_3^- [$a'=3\times3.169=9.507$ Å] is longer than that of AuI_2^- (9.221 Å);[9,18] this is in agreement with the usual relation of the anion length betweenAuI_2^- and I_3^-.[2] Consequently, the anion content determined by $a/a'=0.422$ is smaller than that of (MDT-TSF)$(AuI_2)_{0.436}$.

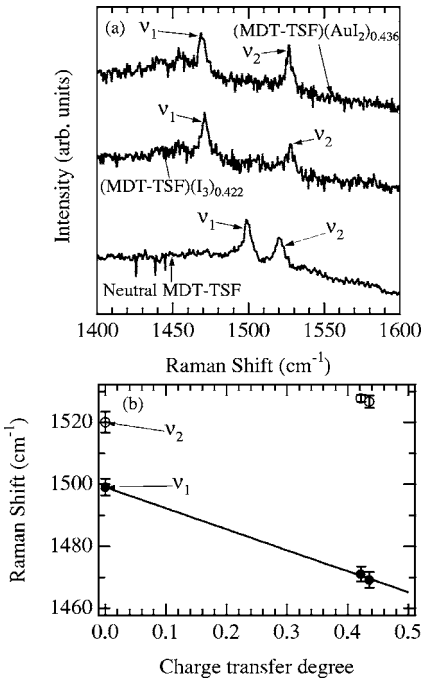

FIG. 3. (a) Raman spectra of MDT-TSF salts and neutral MDT-TSF at room temperature. (b) Charge-transfer degree dependence of the Raman shifts of MDT-TSF salts. The solid line is the fitted result.

The positions of some vibrational modes of the organic conductors are very sensitive to the charge on the organic donor or acceptor molecules. Infrared spectroscopy is not a good tool to investigate these vibration modes due to the strong dispersion of the charge-transfer (CT) band in the infrared region. On the other hand, the CT band does not appear in the Raman spectrum, and electron-phonon coupling does not play an important effect on the position of the a_g mode. Although the central C═C bond stretching between the two five-member rings is very charge sensitive in a TTF molecule (TTF: tetrathiafulvalene), this mode is not Raman active because of the asymmetric shape of the MDT-TSF molecule. Therefore, we have investigated C═C stretching mode along the molecular short axis; i.e., the ring C═C stretching mode.

Figure 3(a) shows the Raman spectra of the neutral MDT-TSF, (MDT-TSF)(AuI$_2$)$_{0.436}$, and (MDT-TSF)(I$_3$)$_{0.422}$. There are two Raman lines. Although the Raman line at 1499 cm^{-1} (ν_1) in the neutral MDT-TSF linearly decreases as the charge-transfer degree (ρ) increases, the Raman line at 1520 cm^{-1} (ν_2) increases with increasing ρ [Fig. 3(b)]. The neutral MDT-TTF molecule, where MDT-TTF is methylenedithio-tetrathiafulvalene, exhibits two strong Raman lines at 1510 and 1551 cm^{-1}; the first line is assigned to the ring C═C bond.[22] This Raman line shifts to 1470 cm^{-1} for κ-(MDT-TTF)$_2$AuI$_2$. This indicates that the Raman shift decreases about 40 cm^{-1}for 0.5 charge-transfer degree. In the BO [BO: bis(ethylenedioxy)tetrathiafulvalene] salts and the ET salts, the Raman shift mainly originating from the ring C═C bond decreases with increasing ρ.[23,24] Therefore, the first Raman line of MDT-TSF, ν_1, comes from the ring C═C bond, and is related to the degree of charge

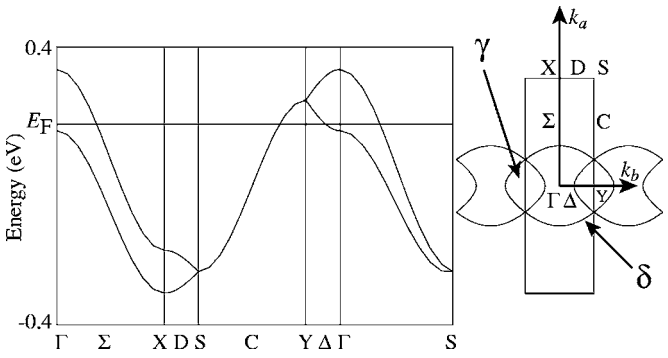

FIG. 4. Energy band structure and the Fermi surface.

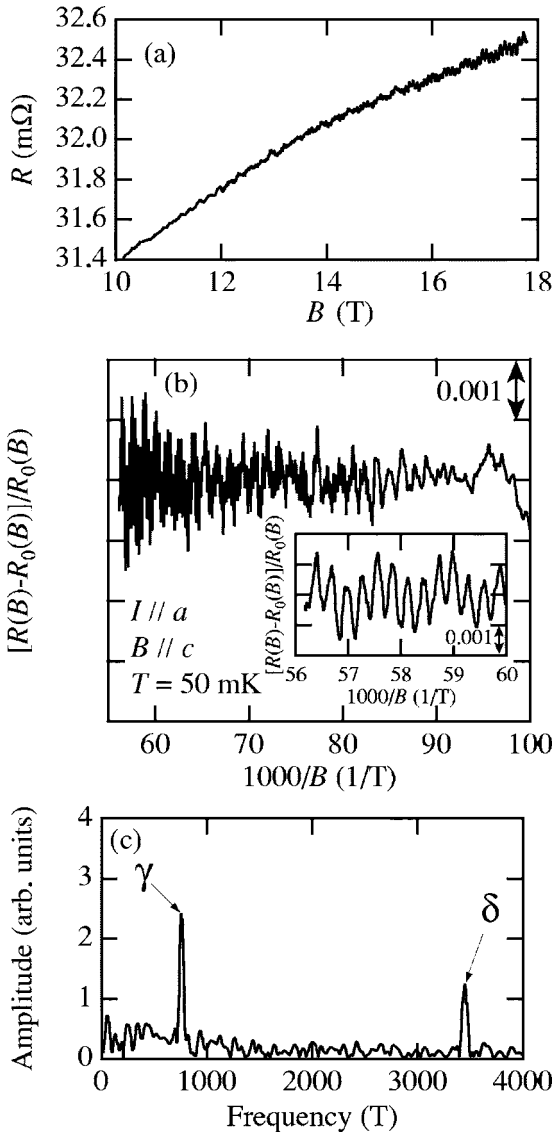

FIG. 5. (a) Magnetoresistance of (MDT-TSF)(I$_3$)$_{0.422}$ at 50 mK ($B\|c$). (b) The SdH signal of the resistance $[R(B)-R_0(B)]/R_0(B)$ for $B\|c$. The inset is the high field region. (c) The FFT spectrum of the SdH oscillation.

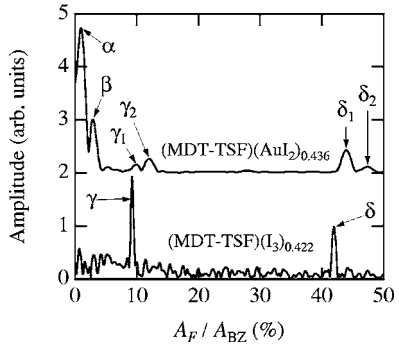

FIG. 6. FFT spectra of the SdH oscillations in $(MDT\text{-}TSF)(AuI_2)_{0.436}$ from Ref. 10 and $(MDT\text{-}TSF)(I_3)_{0.422}$.

transfer as $\nu_1 = 1499 - 67.63\rho$. Although the linewidths of the present Raman spectra are considerably broad, the shift of ν_1 is regarded as the second evidence of the difference of the degree of charge transfer between the AuI_2 and the I_3 salts.

As the definite degree of charge transfer is known, it is possible to calculate the energy band structure without incommensurate anion potential. The calculated transfer integrals are $t_a = 123.5$, $t_{p1} = -6.6$, and $t_{p2} = -37.5$ meV. Figure 4 shows the energy band structure and the Fermi surface calculated on the basis of the tight-binding approximation. The band filling is 0.789, which is a little different from the filling of the AuI_2 salt (0.782). The energy bands are degenerated on the C line owing to the donor lattice symmetry (*Pnma*).[25] Therefore, the Fermi surface (FS) consists of overlapping cylinders. The cross-sectional area of the γ orbit ($A_{F,\gamma}$) is 9.12% and the δ orbit ($A_{F,\delta}$) is 42.2% of the first Brillouin zone (A_{BZ}). It is important that the area of the δ orbit ($A_{F,\delta}/A_{BZ}$) is equal to the degree of charge transfer.

In order to estimate the δ-orbit area experimentally, the SdH oscillation measurements were carried out. Figure 5(a) is the magnetic field dependence of the electrical resistance at 50 mK ($B \| c$). Above 10 T, the magnetoresistance shows oscillating behavior. The oscillatory part (SdH signal) of the resistance represented by $[R(B) - R_0(B)]/R_0(B)$, rescaled by the nonoscillatory background $R_0(B)$, is shown in Fig. 5(b). Figure 5(c) shows the fast Fourier transformation (FFT) spectra. There are two strong peaks γ and δ.

The observed cross-sectional area of the δ orbit ($A_{F,\delta}/A_{BZ} = 42.0\%$) is in agreement with the large cross section estimated from the band calculation. This number is also equal to the amount of charge transfer coming from the anion content 0.422. The observed γ orbit ($A_{F,\gamma}/A_{BZ} = 9.30\%$) is assigned to the 9.12% overlapping area. This is the third piece of evidence that the charge-transfer degree is slightly smaller than that of $(MDT\text{-}TSF)(AuI_2)_{0.436}$ as compared in Fig. 6. Although the energy bands are degenerated on the C line, the incommensurate anion lattice along the *a* axis may destroy this symmetry. This broken symmetry makes the δ orbit a magnetic breakdown orbit that appears only at high fields (>13 T).

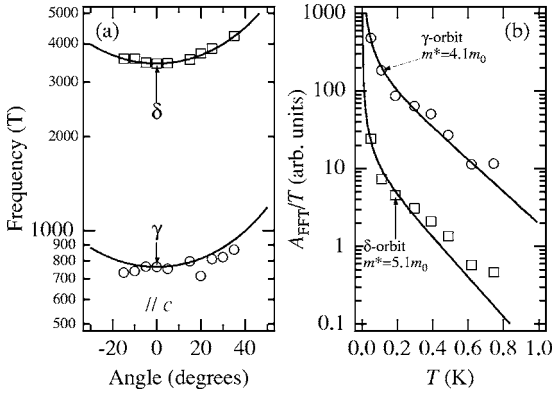

FIG. 7. (a) Field angle dependences of the SdH frequencies and (b) mass plots. The solid lines in (a) show the $1/\cos\theta$ dependences, and the solid lines in (b) are the fitted results.

TABLE I. Shubnikov–de Haas frequency, cross-sectional Fermi-surface area, effective cyclotron mass, and the Dingle temperature for the γ and δ orbits.

Orbit	F (T)	A_F/A_{BZ} (%)	m^*/m_0	T_D (K)
γ	764	9.30	4.1	0.48
δ	3450	42.0	5.1	1.3

As shown in Fig. 7(a), the SdH frequencies roughly show $1/\cos\theta$ behavior expected for quasi-two-dimensional (2D) electronic systems, where θ is the angle between the magnetic field and the *c* axis in the *bc* plane. The obtained frequencies are summarized in Table I with the ratios of the cross-sectional area to the first Brillouin zone based on the donor lattice. The cyclotron radius of the δ orbit at 14 T is estimated as 0.15 μm.

The SdH signals have been analyzed in the conventional way using the Lifshitz-Kosevich (LK) formula for the FFT amplitude, A_{FFT}.[26,27]

Temperature dependences of the oscillation amplitude divided by temperature, so-called mass plots, are presented in Fig. 7(b). The solid lines are the calculated results according to the LK formula. The determined effective cyclotron mass ratios, m^*/m_0 (m_0 is the free electron mass), are listed in Table I. The Dingle temperatures (T_D) simply determined from the field dependence of the oscillations, are also shown in Table I. The Dingle temperatures in Table I for γ and δ give approximately the lower and upper limits, respectively, because the γ and δ orbits are expected to include some Bragg reflection and magnetic breakdown points.

Figure 8 shows the temperature dependence of the electrical resistivity $\rho_{\|a}$. The superconducting transition tempera-

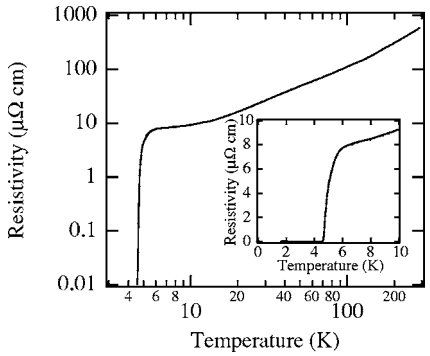

FIG. 8. Temperature dependence of the resistivity. The inset is the low temperature region.

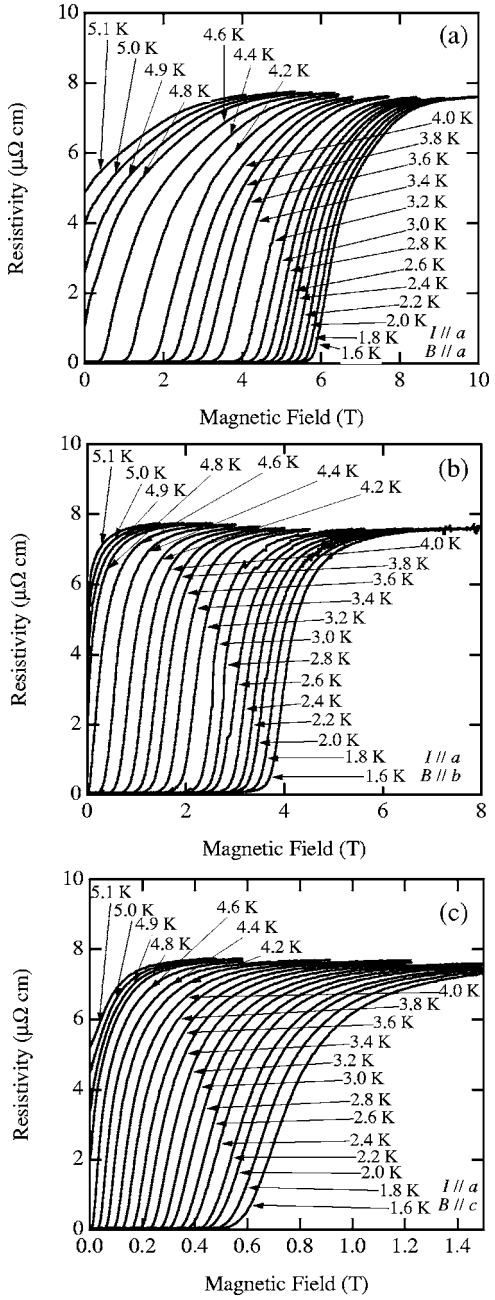

FIG. 9. Magnetic field dependence of resistivity [(a) $B\|a$, (b) $B\|b$, and (c) $B\|c$] under various temperatures.

ture (T_c) is determined as 4.9 K from the midpoint of the resistive transition. This T_c is slightly higher than that of the AuI_2 salt (4.5 K).

Figure 9 presents the magnetic field dependence of the electrical resistivity under various temperatures. The magnetoresistance increases linearly in the normal phase. For $B\|a$, the transition width is considerably broadened with increasing temperature. Figure 10(a) shows the temperature dependence of the upper critical fields of $(MDT\text{-}TSF)(I_3)_{0.422}$, determined from 50% recovery of the extrapolated magnetoresistance from the higher field region in Fig. 9. In several highly two-dimensional superconductors including high-T_c cuprates, the curvature of resistive transition field [$B_{c2}(T)$] is reported to change depending on the definition of

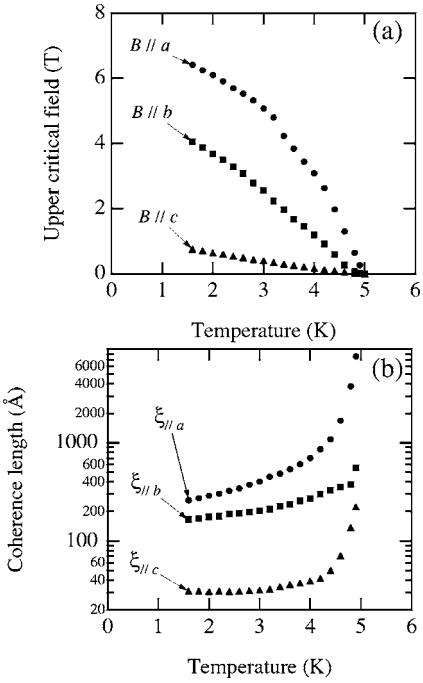

FIG. 10. Temperature dependence of (a) the upper critical fields and (b) the GL coherence lengths.

the recovery percentage, and in the small resistance limit the shape of $B_{c2}(T)$ perpendicular to the conducting sheet approaches to the irreversibility line.[28,29] In the present compound, however, even if B_{c2} is defined by 10 or 90% recovery, the shape of $B_{c2}(T)$ does not change qualitatively.

We can estimate the Ginzburg-Landau (GL) coherence lengths $\xi_{\|a}$, $\xi_{\|b}$, and $\xi_{\|c}$ from the following relation:[30]

$$B_{c2\|i}(T) = \frac{\Phi_0}{2\pi} \frac{1}{\xi_{\|j}(T)\xi_{\|k}(T)}, \tag{1}$$

where Φ_0 is the flux quantum. Figure 10(b) shows the GL coherence lengths for three directions. The coherence lengths

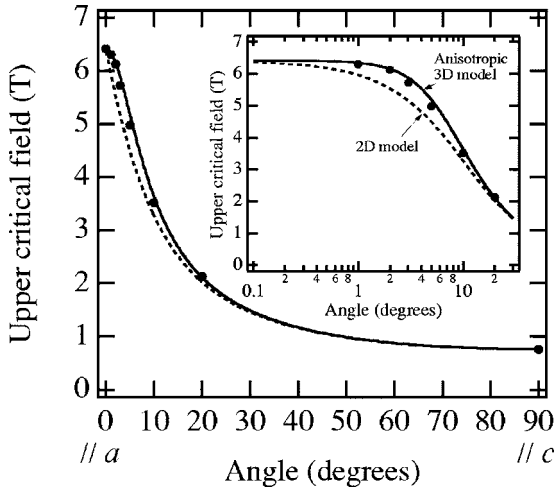

FIG. 11. Angular dependence of the upper critical field on the *ac* plane at 1.6 K. The solid and dotted lines are the calculation based on the anisotropic 3D model and the 2D model, respectively. The inset is the low angle region.

TABLE II. Charge-transfer degree ρ, superconducting transition temperatures T_c, calculated density of states at the Fermi level $N(E_F)$, observed SdH frequencies F_{expt} of the γ and δ orbits, effective cyclotron mass ratios m^*/m_0, the calculated cyclotron mass ratios m_c/m_0, and the ratio between the effective and calculated cyclotron masses m^*/m_c. The total density of states $N(E_F)$ is given in units of (total states) eV^{-1} (donor molecule)$^{-1}$.

Materials	ρ (e)	T_c (K)	$N(E_F)$	F_{expt} (T)	m^*/m_0	m_c/m_0	m^*/m_c
(MDT-TSF)$(I_3)_{0.422}$	0.422	4.9	1.93	764 (γ)	4.1[a]	2.2	1.9
				3450 (δ)	5.1[a]	3.6	1.4
(MDT-TSF)$(AuI_2)_{0.436}$	0.436	4.5	1.95	860 (γ)	2.8[b]	2.1	1.3
				3750 (δ)	4.3[b]	3.6	1.2
(MDT-ST)$(I_3)_{0.417}$	0.417	4.3	2.00	704 (γ)	1.7[c]	2.1	0.81
				3660 (δ)	2.9[c]	3.8	0.76

[a]This work.
[b]Reference 10.
[c]Reference 32.

are $\xi_{\|a}=261$ Å, $\xi_{\|b}=166$ Å, and $\xi_{\|c}=31$ Å at $T=1.6$ K. The in-plane coherence lengths $\xi_{\|a}$ and $\xi_{\|b}$ are much shorter than the cyclotron radius of the δ orbit at 14 T (i.e., 0.15 μm) estimated from the SdH oscillations. Therefore, the present compound is a clean limit superconductor. The transverse coherence length ($\xi_{\|c}$) is longer than the thickness of the conducting sheet [$c/2=12.810(1)$ Å], indicating that the superconductivity is not two dimensional but three dimensional (3D).

Figure 11 shows the field angle dependence of the upper critical fields at 1.6 K. For anisotropic 3D superconductors, the field angle dependence of the upper critical field is

$$\left(\frac{B_{c2}(\theta)\sin\theta}{B_{c2\perp}}\right)^2+\left(\frac{B_{c2}(\theta)\cos\theta}{B_{c2\|}}\right)^2=1, \tag{2}$$

where θ is the angle of the field from the conducting plane ($\|ab$ plane).[30] For 2D superconductors, the angle dependence is changed to the following equation:[30]

$$\left|\frac{B_{c2}(\theta)\sin\theta}{B_{c2\perp}}\right|+\left(\frac{B_{c2}(\theta)\cos\theta}{B_{c2\|}}\right)^2=1. \tag{3}$$

The difference between the 3D and 2D models is large near $\theta=0^\circ$; the 2D curve has a cusp at the magnetic field parallel to the conducting sheet. The observed upper critical fields ($B_{c2\|}$ and $B_{c2\perp}$) are well reproduced by the anisotropic 3D model (Fig. 11). (MDT-TSF)$(I_3)_{0.422}$ is recognized as a highly anisotropic 3D superconductor, similarly to the other organic superconductors based on MDT-TTF derivatives, (MDT-TSF)$(AuI_2)_{0.436}$,[9] (MDT-ST)$(I_3)_{0.417}$,[14] and κ-(MDT-TTF)$_2AuI_2$.[31] In spite of the entirely different donor arrangement, κ-(MDT-TTF)$_2AuI_2$ also has a three-dimensional character. Anisotropic 3D superconductivity is characteristic of the MDT-TSF family donors in general.

IV. DISCUSSION

In the SdH measurements, only two orbits, γ and δ orbits, are observed in (MDT-TSF)$(I_3)_{0.422}$. For (MDT-TSF)$(AuI_2)_{1.266}$, the Fermi surface reconstructed by the third harmonic incommensurate anion potential $3\boldsymbol{q}=3\rho\boldsymbol{a}^*$ has been observed, where ρ is equal to the degree of charge transfer: 0.436.[10] This characteristic reconstruction is related to the intensity of the anion sublattice reflections observed in the x-ray oscillation photograph. The x-ray $3\boldsymbol{q}$ intensities are even stronger than the other $n\boldsymbol{q}$ spots' intensities, where n is an integer. The same FS reconstruction has been also observed in the incommensurate organic superconductor (MDT-ST)$(I_3)_{0.417}$. The incommensurate potential is significantly smaller than that made by the donor molecules and the conduction electrons perturbatively feel the incommensurate potential.

Judging from the x-ray experiments, the dominant sublattice potential is given by $3\boldsymbol{q}=3\times0.422\boldsymbol{a}^*$ vector in the present compound.[18] The vector $3\boldsymbol{q}$ is associated with the average distance of I-I (3.169 Å at room temperature) in the real space. Our previous results require that the FS is reconstructed by $3\boldsymbol{q}$, and the new closed orbit, i.e., the β orbit in the AuI_2 salt, with $F\sim520$ T should be observed. However, our experimental result does not show such an extra orbit. This indicates that the interaction between the donor molecules and the incommensurate anion potential is extremely small, and the conduction electrons do not perturbatively feel the incommensurate potential.

The superconducting transition temperature of (MDT-TSF)$(I_3)_{0.422}$ is slightly higher than that of (MDT-TSF)$(AuI_2)_{1.266}$. For the BCS type superconductors, the critical temperature is given by the following equation:

$$T_c=1.13\Theta_D\exp\left(\frac{-1}{N(E_F)V}\right), \tag{4}$$

where Θ_D is the Debye temperature, $N(E_F)$ is the density of states at the Fermi level, and V is an attracting potential.[30] This BCS formula indicates that the larger $N(E_F)$ and Θ_D gives the higher T_c. As shown in Table II, however, the calculated $N(E_F)$ of the I_3 salt is smaller than that of the AuI_2 salt, in disagreement with Eq. (4). Figure 12 shows the calculated density of states of (MDT-TSF)$(I_3)_{0.422}$. There are two sharp van Hove singularity (VHS) peaks below E_F, which are related to the saddle points of the band at Γ and X

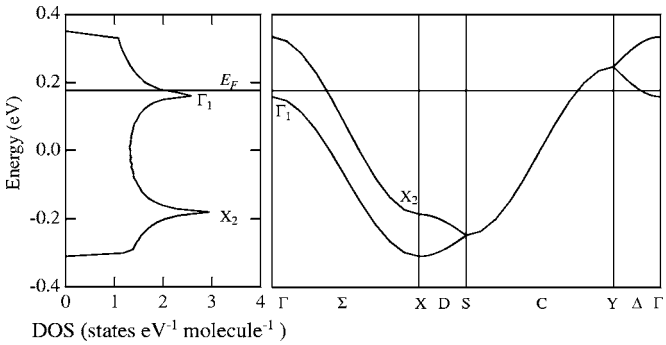

FIG. 12. Calculated density of states of $(MDT\text{-}TSF)(I_3)_{0.422}$.

points, respectively. Therefore, $N(E_F)$ increases with decreasing the band filling (or increasing the charge transfer degree) above the upper VHS level. This tendency appears for the present superconductors in Table II, independent of the small difference of the band width. Although we cannot determine the Debye temperature from the present results, several organic superconductors with different T_c have the same Debye temperature $\Theta_D \sim 210$ K, for κ-$(ET)_2X$ $\{X=CuN[(CN)_2]Br$ $(T_c=11.8$ K), $Cu(NCS)_2$ $(T_c=10.4$ K), and I_3 $(T_c=3.6$ K)$\}$.[33] Therefore, we speculate that our present compounds have a similar Θ_D in spite of the different T_c.

Although the cross-sectional area of the FS of the I_3 salt is smaller than that of the AuI_2 salt, the effective cyclotron masses of the γ and δ orbits estimated from the SdH oscillations of the I_3 salt are heavier than those of the AuI_2 salt, as shown in Table II. In κ-$(ET)_2Cu(NCS)_2$ and α-$(ET)_2NH_4Hg(SCN)_4$, the high-pressure SdH investigations show that the higher T_c state has the heavier effective cyclotron mass.[34,35]

The bare cyclotron mass m_c is associated with the cyclotron frequency ω_c by

$$\omega_c = \frac{eB}{m_c}. \tag{5}$$

This mass is related to the average of the dispersion relation along the periodic orbit:

$$m_c = \frac{\hbar^2}{2\pi}\frac{\partial A_F(E_F)}{\partial E_F}, \tag{6}$$

where $A_F(E_F)$ is the cross section of the FS defined by the orbit described by an electron or hole, in the presence of a magnetic field B.[36] The cyclotron mass is experimentally determined by the mass plots, as shown in Fig. 7(b). The experimentally determined mass includes not only the band dispersion but also all interactions, i.e., electron-phonon and electron-electron interactions. Therefore, we have written the observed effective cyclotron mass as m^* to distinguish the bare cyclotron mass m_c.

In a 2D electronic system, the bare cyclotron mass is written as

$$m_c = 2\pi\hbar^2\rho_c(E_F), \tag{7}$$

where $\rho_c(E_F)$ is the 2D density of states of the cyclotron orbit.[37] Following Merino and McKenzie,[37] the observed effective cyclotron mass is given by

$$m^* = 2\pi\hbar^2\tilde{\rho}_c(\tilde{E}_F), \tag{8}$$

where a tilde denotes renormalized quantities. This relation gives

$$m^* = 2\pi\hbar^2\rho_c(E_F)/Z = m_c/Z, \tag{9}$$

where Z is the quasiparticle weight. Therefore, the ratio $m^*/m_c = 1/Z$ means the magnitude of the interaction. We can estimate this parameter by the ratio between the effective cyclotron mass determined by the SdH oscillations and the bare cyclotron mass estimated by Eq. (6) from the band calculation.[38] The calculated results, m_c/m_0 and m^*/m_c, are also listed in Table II. The obtained m^*/m_c increases with increasing T_c. This tendency shows us that the mass enhancement (i.e., a strong many-body effect) is the major factor that increases T_c. For other organic superconductors based on ET, we have found a similar relation in between T_c and m^*/m_c, as will be reported shortly.[38] In the present MDT-TSF salts, the differences between the AuI_2 and the I_3 salt are the band filling, the transfer integral t, and the superconducting transition temperature T_c. The on-site Coulomb repulsion U will be the same because of the same donor molecule with the basically same crystal structure. The strength of the electronic correlation is strongly related to the ratio U/t. One transfer integral (t_{p1}) of the I_3 salt is about half of that of the AuI_2 salt. Therefore, the difference between the observed cyclotron mass originates in the electron-electron interaction. However, the correlation between T_c and m^* in the MDT-TSF salts is not as strong as that in κ-$(ET)_2Cu(NCS)_2$.[34]

V. CONCLUSION

The Raman spectra and SdH oscillations have provided clear evidence that the degree of charge transfer is 0.422, i.e., $(MDT\text{-}TSF)(I_3)_{0.422}$. The long coherence length perpendicular to the conducting sheet and the angle dependence of the upper critical field demonstrate that $(MDT\text{-}TSF)(I_3)_{0.422}$ is an anisotropic three-dimensional superconductor. Although the superconducting transition temperature of this compound is slightly higher than that of $(MDT\text{-}TSF)(AuI_2)_{0.436}$, the present compound has the smaller charge transfer degree, smaller density of states, and heavier cyclotron mass than those of the AuI_2 salt. These results suggest that the many-body interaction is important to increase the superconducting transition temperature.

ACKNOWLEDGMENTS

This work was partially supported by a Grant-in-Aid for Young Scientists (B) (Grant No. 17750176) and Grants-in-Aid for Scientific Research on Priority Areas of Molecular Conductors (Grant Nos. 15073211, 15073218, and 15073225) from MEXT.

[1] T. Ishiguro, K. Yamaji, and G. Saito, *Organic Superconductors*, 2nd ed. (Springer, Berlin, 1998).
[2] J. M. Williams, J. R. Ferraro, R. J. Thorn, K. D. Carlson, U. Geiser, H. H. Wang, A. M. Kini, and M.-H. Whangbo, *Organic Superconductors (Including Fullerenes)* (Prentice-Hall, Englewood Cliffs, NJ, 1992).
[3] For a review about organic conductors with unusual band fillings, see T. Mori, Chem. Rev. (Washington, D.C.) **104**, 4947 (2004).
[4] R. Kumai, A. Asamitsu, and Y. Tokura, J. Am. Chem. Soc. **120**, 8263 (1998).
[5] H. Mori, M. Kamiya, M. Haemori, H. Suzuki, S. Tanaka, Y. Nishio, K. Kajita, and H. Moriyama, J. Am. Chem. Soc. **124**, 1251 (2002).
[6] M. Katsuhara, S. Kimura, T. Mori, Y. Misaki, and K. Tanaka, Chem. Mater. **14**, 458 (2002).
[7] H. M. Yamamoto and R. Kato, Chem. Lett. (**2000**) 970.
[8] K. Takimiya, Y. Kataoka, Y. Aso, T. Otsubo, H. Fukuoka, and S. Yamanaka, Angew. Chem., Int. Ed. **40**, 1122 (2001).
[9] T. Kawamoto, T. Mori, K. Takimiya, Y. Kataoka, Y. Aso, and T. Otsubo, Phys. Rev. B **65**, 140508(R) (2002).
[10] T. Kawamoto, T. Mori, C. Terakura, T. Terashima, S. Uji, K. Takimiya, Y. Aso, and T. Otsubo, Phys. Rev. B **67**, 020508(R) (2003).
[11] T. Kawamoto, T. Mori, C. Terakura, T. Terashima, S. Uji, H. Tajima, K. Takimiya, Y. Aso, and T. Otsubo, Eur. Phys. J. B **36**, 161 (2003).
[12] K. Takimiya, A. Takamori, Y. Aso, T. Otsubo, T. Kawamoto, and T. Mori, Chem. Mater. **15**, 1225 (2003).
[13] T. Kawamoto, T. Mori, S. Uji, J. I. Yamaura, H. Kitagawa, A. Takamori, K. Takimiya, and T. Otsubo, Phys. Rev. B **71**, 172503 (2005).
[14] T. Kawamoto, T. Mori, T. Terashima, S. Uji, K. Takimiya, A. Takamori, and T. Otsubo, J. Phys. Soc. Jpn. **74**, 1529 (2005).
[15] K. Takimiya, M. Kodani, N. Niihara, Y. Aso, T. Otsubo, Y. Bando, T. Kawamoto, and T. Mori, Chem. Mater. **16**, 5120 (2004).
[16] T. Kawamoto, Y. Bando, T. Mori, K. Takimiya, and T. Otsubo, Phys. Rev. B **71**, 052501 (2005).
[17] R. N. Lyubovskaya, E. I. Zhilyaeva, S. I. Pesotskiĭ, R. B. Lyubovskiĭ, L. O. Atovmyan, O. A. D'yachenko, and T. G. Takhirov, JETP Lett. **46**, 188 (1987).
[18] K. Takimiya, M. Kodani, Y. Kataoka, Y. Aso, T. Otsubo, T. Kawamoto, and T. Mori, Chem. Mater. **15**, 3250 (2003).
[19] T. J. Marks and D. W. Kalina, in *Extended Linear Chain Compounds*, edited by J. S. Miller (Plenum, New York, 1983), Vol. I, Chap. 6; P. Coppens, *ibid*. edited by J. S. Miller (Plenum, New York, Chap. 7.
[20] T. Mori, A. Kobayashi, Y. Sasaki, H. Kobayashi, G. Saito, and H. Inokuchi, Bull. Chem. Soc. Jpn. **57**, 627 (1984).
[21] We have calculated the overlap integrals without S 3*d* and Se 4*d* orbitals on the basis of the results of (MDT-TSF)$(AuI_2)_{0.436}$ reported in Refs. 10 and 11.
[22] J. S. Zambounis, A. P. Patsis, E. I. Kamitsos, C. W. Mayer, and G. C. Papavassiliou, and J. Raman, J. Raman Spectrosc. **26**, 9 (1995).
[23] O. Drozdova, H. Yamochi, K. Yakushi, M. Uruichi, S. Horiuchi, and G. Saito, J. Am. Chem. Soc. **122**, 4436 (2000).
[24] K. Yamamoto, K. Yakushi, K. Miyagawa, K. Kanoda, and A. Kawamoto, Phys. Rev. B **65**, 085110 (2002).
[25] G. F. Koster, Solid State Phys. **5**, 173 (1957).
[26] D. Shoenberg, *Magnetic Oscillations in Metals* (Cambridge University Press, Cambridge, 1984).
[27] J. Wosnitza, *Fermi Surfaces of Low Dimensional Organic Metals and Superconductors* (Springer, Berlin, 1996).
[28] W. K. Kwok, U. Welp, K. D. Carlson, G. W. Crabtree, K. G. Vandervoort, H. H. Wang, A. M. Kini, J. M. Williams, D. L. Stupka, L. K. Montgomery, and J. E. Thompson, Phys. Rev. B **42**, R8686 (1990).
[29] Y. Ando, G. S. Boebinger, A. Passner, L. F. Schneemeyer, T. Kimura, M. Okuya, S. Watauchi, J. Shimoyama, K. Kishio, K. Tamasaku, N. Ichikawa, and S. Uchida, Phys. Rev. B **60**, 12475 (1999).
[30] M. Tinkham, *Introduction to Superconductivity*, 2nd ed. (McGraw-Hill, New York, 1996).
[31] K. Kanoda, K. Kato, Y. Kobayashi, M. Kato, T. Takahashi, K. Oshima, B. Hilti, and J. Zambounis, Synth. Met. **55-57**, 2871 (1993).
[32] T. Kawamoto, T. Mori, K. Enomoto, T. Konoike, T. Terashima, S. Uji, A. Takamori, K. Takimiya, and T. Otsubo, Phys. Rev. B **73**, 024503 (2006).
[33] For the CuN[$(CN)_2$]Br salt, see B. Andraka, C. S. Jee, J. S. Kim, G. R. Stewart, K. D. Carlson, H. H. Wang, A. V. S. Crouch, A. M. Kini, and J. M. Williams, Solid State Commun. **79**, 57 (1991); For the $Cu(NCS)_2$ salt, see B. Andraka, J. S. Kim, G. R. Stewart, K. D. Carlson, H. H. Wang, and J. M. Williams, Phys. Rev. B **40**, R11345 (1989); For the I_3 salt, see J. Wosnitza, X. Liu, D. Schweitzer, and H. J. Keller, *ibid.* **50**, 12747 (1994).
[34] J. Caulfield, W. Lubczynski, F. L. Pratt, J. Singleton, D. Y. K. Ko, W. Hayes, M. Kurmoo, and P. Day, J. Phys.: Condens. Matter **6**, 2911 (1994).
[35] J. S. Brooks, X. Chen, S. J. Klepper, S. Valfells, G. J. Athas, Y. Tanaka, T. Kinoshita, N. Kinoshita, M. Tokumoto, H. Anzai, and C. C. Agosta, Phys. Rev. B **52**, 14457 (1995).
[36] J. M. Ziman, *Principles of the Theory of Solids*, 2nd ed. (Cambridge University Press, Cambridge, 1972).
[37] J. Merino and R. H. McKenzie, Phys. Rev. B **62**, 2416 (2000).
[38] T. Kawamoto and T. Mori (in preparation).